# Seismic earth pressure on a multi-story underground structure

†\*Z.Y. Chen<sup>1,2</sup>, W. Chen<sup>3</sup>, and H. Fan<sup>3</sup>

\*Presenting author: zhiyichen@tongji.edu.cn †Corresponding author: zhiyichen@tongji.edu.cn

#### **Abstract**

For a multi-story underground structure, distribution and amplitude of seismic earth pressure along its side wall depth during an earthquake are critical for seismic design and safety evaluation. In this paper, a series of 1-g shaking table tests were conducted on a four-story subway station firstly. Experimental results showed that the distribution of maximum lateral dynamic earth pressure appeared an "S" shape, which was distinguished from that of a single-story underground structure. In the latter case, it is generally in a form of a triangle distribution. Furthermore, parametric study was carried out through nonlinear dynamic time history analyses using the general purpose finite element code ABAQUS. Attention was paid on influences of types of soils, structural stiffness, and vertical earthquake component on the distribution of seismic earth pressure. Numerical results showed that structures surrounded by sand suffered larger dynamic earth pressure than that those surrounded by clay. Peak dynamic earth pressure of a flexible structure was a little smaller than that of a rigid one. And vertical earthquake component excited lateral dynamic earth pressure in some degree.

**Keywords:** Seismic earth pressure, Multi-story underground structure, Shaking table test, Parametric study, Stiffness

#### Introduction

Nowadays, with the rapid development of economy and society modern underground transportation, represented by the subway, has become popular. In China under the current plan, 36 cities were approved to build rail transit, and it is planning to reach 6000 km of rail transit by 2020 [Sun (2013)]. At the same time, the world has experienced a high incidence of earthquakes. The M 9.1 earthquake in Sumatra in 2004, the M 8.0 earthquake in Wenchuan, China in 2008, and the M 9.0 earthquake in the northeast of Japan in 2011 all caused a great loss of human life and property. Obviously, strong earthquakes heavily threaten underground subways those are building or built. Typical lateral design of foundation systems and retaining structures often relies on static earth pressure theories and tends to neglect seismic effects frequently due to the lack of understanding thereof and the shortcoming of experimental data. While this assumption can be accurate for foundation systems exposed to small levels of seismic shaking, stronger accelerations due to larger magnitude earthquakes can cause significant damage to the foundations and superstructures [Luu (2013)].

Hence, theoretical, numerical and experimental studies of seismic earth pressure on underground structures had been conducted in recent years. Wang et al. [2010] proposed a new method to calculate the seismic earth pressure of shallow buried underground structures by combining Xie theory and M-O formula. Ostadan [2005] conducted a series study on seismic soil structure interaction of building walls resting

<sup>&</sup>lt;sup>1</sup> Associate professor, Department of Geotechnical Engineering, Tongji University, Shanghai, China.

<sup>2</sup> State Key Laboratory of Disaster Reduction in Civil Engineering, Shanghai, China.

<sup>&</sup>lt;sup>3</sup> Master candidate, Department of Geotechnical Engineering, Tongji University, Shanghai, China.

on firm foundation materials and proposed a simplified method for predicting the maximum seismic pressures. Gazetas et al. [2004] carried out a numerical study of dynamic stresses imposed on a variety of retaining systems under short-duration and impulsive base excitation. Psarropoulos et al. [2005] developed a general finite-element method that specifically focused on the distribution of dynamic earth pressures on rigid and flexible walls. Shaking table test and centrifuge test are popular to study the dynamic soil structure interaction. Yang et al. [2003] conducted shaking table tests on a double-story subway station and found that the dynamic lateral earth pressures were large at the middle part and small at the top and bottom. Madabhushi and Zeng [2007] conducted centrifuge tests to investigate the seismic response of a cantilever retaining wall under earthquake loading and pointed that the effect of an earthquake was more severe on a cantilever retaining with saturated backfill than that with dry backfill.

However, amounts of studies are almost aimed at retaining structures. There are still some differences between retaining structures and underground subway structures, such as design structural parameters, boundary conditions, and stress conditions. Hence it is not appropriate to simply apply the computational methods for retaining structures to subway structures. Furthermore, most researches aimed at traditional subway structure, which was single story or double story. Owing to new requirements on functions of underground space, modern subway station developing towards having a multilevel and complex structural form. With the increase of layers, lateral stiffness of stations decreases significantly, which changes the distribution and amplitude of seismic earth pressures.

In this study, a series of 1-g shaking table tests were conducted on a four-story subway station firstly. Due to the lacking of resources and time, many influence factors cannot be considered in tests. Thus, the experimental results are used to confirm the ability of the numerical technique to simulate the dynamic earth pressure. Then study was carried out through nonlinear dynamic time history analyses using the general purpose finite element code ABAQUS. Influences of types of soils, structural stiffness, and horizontal and vertical earthquake components on the distribution of seismic earth pressure were studied.

#### **Shaking table tests**

## Experimental setup

The shaking table test was carried out using the MTS Company shaking table facility at the State Key Laboratory for Disaster Reduction in Civil Engineering, Tongji University. The table can be input with three-dimensional and six-degree-of-freedom motions. The dimensions of the table are 4 m  $\times$  4 m. The working frequency ranges from 0.1 to 50 Hz. The shaking table vibrates with two maximum horizontal direction accelerations of 1.2 g and 0.8 g, and a maximum acceleration of 0.7 g vertically. A flexible container was used in the test. The cylindrical soil container was 3000 mm in diameter. Figure 1 shows the shaking table and the soil container.



Figure 1. Shaking table and soil container

## Scale factor design and materials

The prototype design of the model structure is a modern subway station with height of 28.3 m. The station was designed originally to be a six-story island platform station, and then because of the need for parking, the first to third floors underground were merged into one layer to function as a stereo garage. The second floor is the lobby floor, the third is a floor that houses equipment, and the fourth is an island platform. The total length of the station is 155 m, and the width varies from 23.6 to 28.35 m.

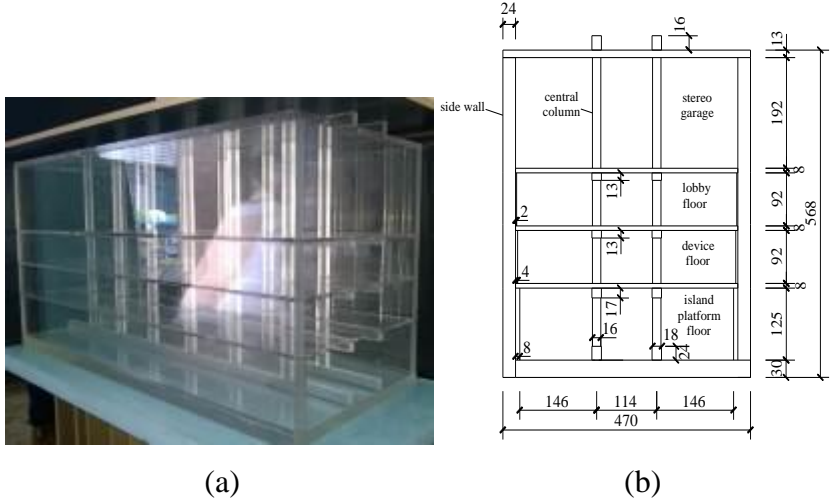


Figure 2. (a) The model structure and (b) its dimensions

On account of the differences in dimensions between a modern subway station and typical station, the scale factor design should be based on the size and bearing capacity of the shaking table, size of the soil container, boundary effect, and convenience of model manufacturing. The geometric scale factor is set to 1:50. Figure 2 shows the model structure and its dimensions. Scale factors among the physical quantities can be deduced using the Buckingham  $\pi$  law:

$$\begin{cases}
S_{\sigma} = S_{E} \\
S_{t} = S_{E}^{\frac{1}{2}} S_{l} S_{\rho}^{\frac{1}{2}} \\
S_{v} = S_{E}^{\frac{1}{2}} S_{\rho}^{\frac{1}{2}} \\
S_{a} = S_{E} S_{l}^{1} S_{\rho}^{1}
\end{cases} , \tag{1}$$

where  $S_{\sigma}$ ,  $S_{E}$ ,  $S_{I}$ ,  $S_{V}$ ,  $S_{a}$  denote the stress scale factor, elastic modulus scale factor, time scale factor, geometric scale factor, velocity scale factor, and acceleration scale factor, respectively. Table 1 shows the scale factors of the model structure.

Table 1. Scale factors of the model structure

Type	Physical quantity	Scale factor
Material properties	Stress	0.106
	Strain	1.000
	Elastic modulus	0.106
	Poisson's ratio	1.000
	Equivalent density	1.765
Geometry properties	Length	0.020
	Linear displacement	0.020
	Angular displacement	1.000
	Area	$4.00 \times 10^{-4}$
Loading	Force	$4.24 \times 10^{-5}$
	Linear load	$2.12 \times 10^{-3}$
	Area load	0.106
	Moment	$8.48 \times 10^{-7}$
Dynamic properties	Mass	$1.41 \times 10^{-5}$
	Stiffness	$2.12 \times 10^{-3}$
	Duration	$8.16 \times 10^{-2}$
	Frequency	12.253
	Velocity	0.245
	Acceleration	3.003

Organic glass was chosen as the material of the model structure owing to its good homogeneity, high strength and low elastic modulus, providing flexibility to the design of the scale factor. This material is also suited to accurate manufacturing. The elastic modulus of three specimens were 3.60, 3.21, and 3.19 MPa, respectively. The average value was 3.33 MPa.

The synthetic model soil was a mixture of sand and sawdust. According to trial tests, adding sawdust to sand can reduce both the density and dynamic shear modulus, which complies with similitude requirements. Employing the Buckingham  $\pi$  law, the scale factors of geometry, density, shear modulus, and inertial acceleration were selected as essential parameters and adjusted to satisfy

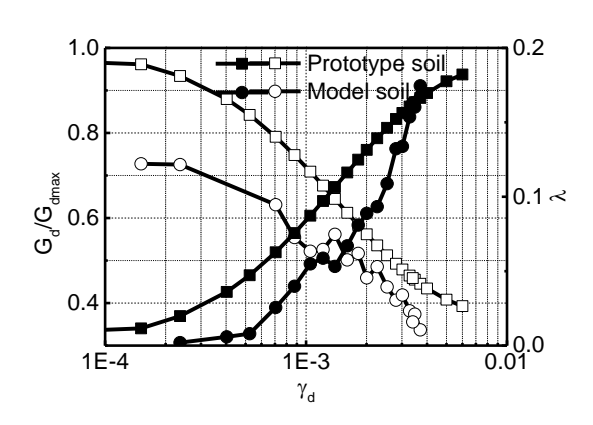
$$S_G/(S_l \bullet S_\rho) = S_a \tag{3}$$

where  $S_G$ ,  $S_I$ ,  $S_\rho$ ,  $S_a$  denote the shear modulus ratio, geometry ratio, density ratio, and inertial acceleration ratio, respectively. The scale factors of soil are presented in Table 2.

Table 2. Scale factors of the model soil

Physical quantity	Symbols	Scale factor
Shear modulus	$S_G$	0.020
Length	$S_{\scriptscriptstyle L}$	0.020
Density	$S_{ ho}$	0.333
Acceleration	$S_a$	3.003

To satisfy the scale factor equation and taking the maximum dynamic shear modulus,  $G_d/G_{d\,\mathrm{max}}-\gamma_d$  curve, and  $\lambda-\gamma_d$  curve into consideration, the most appropriate mass ratio of sawdust to sand was 1:2.5, where  $G_d, G_{d\,\mathrm{max}}, \lambda, \gamma_d$  denote the dynamic shear modulus, maximum dynamic shear modulus, damping ratio, and dynamic shear strain respectively. The density of the mixture was 0.7 kg/m³, the density scale factor was 0.39, the confining pressure ratio was 0.02, and the modulus obtained in the test was 1.81 MPa. The  $G_d/G_{d\,\mathrm{max}}-\gamma_d$  curve and  $\lambda-\gamma_d$  curve obtained in a dynamic triaxial test are presented in Figure 3.



P: Soil pressure gauge

P1

P2

P2

P3

P4

P4

P6

P7

P1

P8

Figure 3. Dynamic properties of the model soil

Figure 4. Layouts of soil pressure meters

### Layout of sensors

The layouts of ten soil pressure gauges attached at the side wall of the model structure are shown in Figure 4. Soil pressure gauges P1–P8 were arranged to explore the distribution of the dynamic earth pressure and P9 and P10 were used to check the dynamic earth pressure.

#### Test schema

For the purpose of investigating the dynamic earth pressure under different intensities and types of ground motions, the three ground motions were scaled to two levels, 0.2 g and 0.6 g. Table 3 gives test cases.

Table 3. Test program

Case	Test case	Ground motion	Horizontal peak acceleration (g)	
1	El-0.2g	El Centro	0.2	
2	El-0.6g	El Centro	0.6	
3	Chi-0.6g	ChiChi	0.6	
4	Shw-0.6g	Shanghai wave	0.6	

### Results from shaking table tests

For convenience, data obtained from tests were converted from model to prototype according to scale factors listed in Table 1. Figure 5(a) shows the peak dynamic lateral earth pressure along the side wall with different types of ground motions. It can be seen that, the amplitude of dynamic earth pressure closely related to ground

motions. Dynamic earth pressures amplitude under ChiChi ground motions were larger than the other. Specifically, the average peak dynamic earth pressure under ChiChi motion was 1.8 times the value under Shanghai wave. It is due to the pulse-like effect [Chen et al. (2015)]. But the distribution patterns were similar. Under three ground motions, the distribution of peak lateral dynamic earth pressure appeared an "S" shape, which was distinguished from that of a single-story underground structure. In the latter case, it is generally in a form of a triangle distribution. This may be because of the large height of the structure.

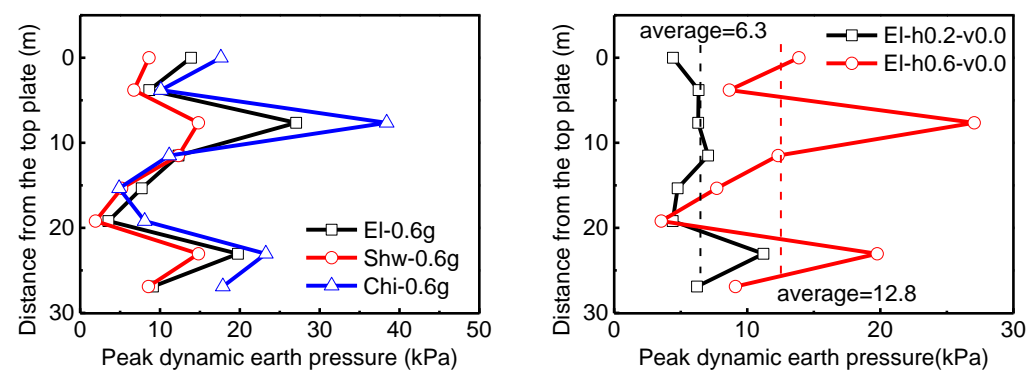


Figure 5. Peak dynamic lateral earth pressure (a) with different types of ground motions; (b) with different peak horizontal accelerations

Figure 5(b) shows the influence of peak horizontal acceleration on the dynamic earth pressures. It is noted that the dash lines in the figure indicated the average values of pressures. It is found that with the increase of the magnitude of the earthquake, dynamic earth pressure increased remarkably. The average value of Case 3 was 2 times the value of Case 1. The influence of peak horizontal acceleration on pressure was different in each measurement point. But whether under a small earthquake or a large one, the distribution both appeared an "S" shape.

## Nonlinear dynamic time history analysis model

Due to the lacking of time and resources, it is difficult to identify many influences factors. For instance, the relative stiffness of soils to structures is an important factor in the soil-structure interaction, but during the test process it is hard to change overall soils or structures without disturbing the soils. Hence, experimental results were used to confirm the ability of the numerical technique to simulate the dynamic earth pressure. And numerical simulation can be used to study influences of the structural stiffness and types of surrounding soils on the distribution of seismic earth pressure.

As shown in Figure 6, the plane strain model was chosen with dimensions of 1000 m long and 85 m high. In order to decrease the influence caused by seismic reflection, infinite element was imposed to the lateral boundaries. The horizontal and vertical displacements were fixed at the bottom. The structure was assumed to exhibit an elastic behavior throughout the entire analysis. Thus concrete in the structure was modeled as a linear elastic material, with unit weight 25kN/m3, Poisson's ratio 0.15 and Young's modulus 24GPa. Actual spacing of the column was taken into consideration with the reduced stiffness. The Mohr-Coulomb model was adopted to simulate soils. Soils were divided into 14 layers and soil properties were obtained from geotechnical investigations. 4-nodes plane strain element (CPE4R) and

quadrilateral plane strain infinite element (CINPE4) were adopted for soil, and beam element (B21) for structure. The interface between structure and ground was modeled as a frictional surface whose contact was assumed to follow the Coulomb friction law. A coefficient of friction equal to 0.4 was assumed which corresponds to a friction angle of 22 degrees.

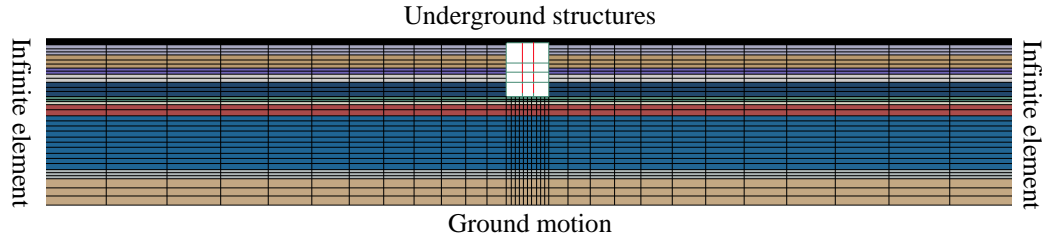


Figure 6. Numerical model of the four-story subway station

El Centro record was used as the input ground motion, which was also the motion used in shaking table test. Figure 7 shows the motion and its Fourier spectrum.

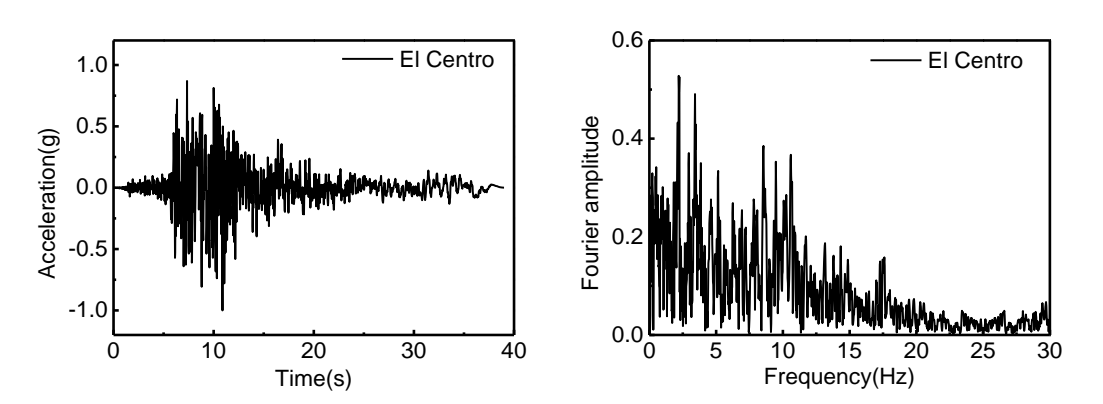


Figure 7. Acceleration time history and Fourier spectrum of El Centro record

## Parametric study

Comparison between numerical and test results

To verify the reliability and accuracy of the numerical model. A nonlinear dynamic time history analysis model was established in consistent with the dimensions of shaking table tests using the above-mentioned method. Figure 8 shows the comparison between numerical and test results in Case 3 (El-h0.6-v0.0). It can be seen that the distribution of dynamic earth pressure obtained from numerical results was also close to an "S" shape. The distributions were different in some degree. This may be due to the constitutive model of the model soil. The Mohr-Coulomb model is more appropriate for prototype soil rather than the synthetic model soil made of sand and sawdust. It is noted that the average dynamic pressure of numerical and test results were close. The error was 5.5%, respectively. Hence, the numerical model is able to investigate the amplitude of pressure in parametric studies.

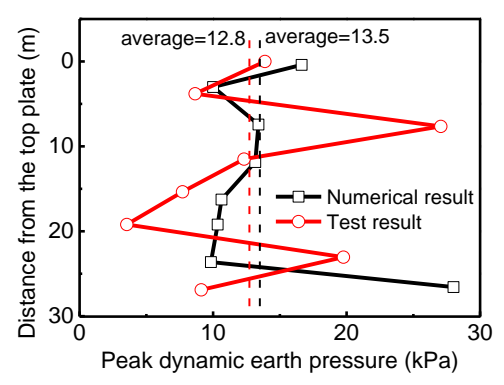


Figure 8. Comparison between numerical and test results in Case 3

The ratio of dynamic earth pressure to static pressure

Figure 9 shows the ratio of dynamic to static pressure under two levels of the earthquake. Firstly, it can be seen that with the increase of peak acceleration, dynamic earth pressure increased notably. Then the ratio at the top of the structure was much larger than that at the bottom. It is because the static earth pressure at top was much smaller than that at the bottom. It is worth noting that at the lower part of the structure, the degree of increase was close. Specifically, ratios under two levels were about 0.15 and 0.27, respectively. It means that when the peak horizontal acceleration was 0.2 g, the lateral earth pressure increased nearly thirty percent, which needed attention in practice.

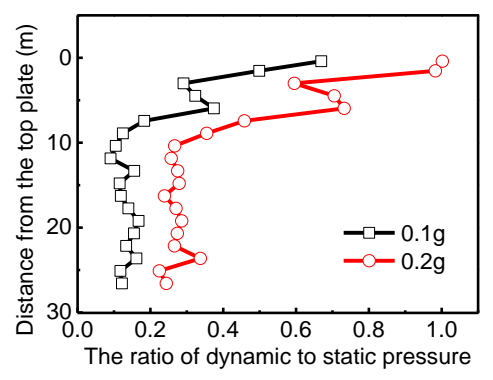


Figure 9. The ratio of dynamic earth pressure to static earth pressure

## Soil types

In order to study the influence of soil type, the second layer to the eighth layer of prototype soils were combines as one homogeneous soil layer. And this layer was defined as sand layer and clay layer in two models, respectively. Frictional angle and cohesion of clay were 16 degrees and 17 kPa, and values of sand were 35 degrees and 0. Figure 10(a) shows the influence of soil type under two levels of the earthquake. It is seen that when the earthquake was small, distributions of dynamic earth pressure were close to linear one in most parts of the structure; when the earthquake was large, distributions in the sand tend to be the "S" shape. Structures surrounded by sand suffered larger dynamic earth pressure than that by clay. Specifically, when peak horizontal acceleration was 0.2 g in clay, dynamic earth pressure was very close to that in the sand when peak acceleration was 0.1 g.

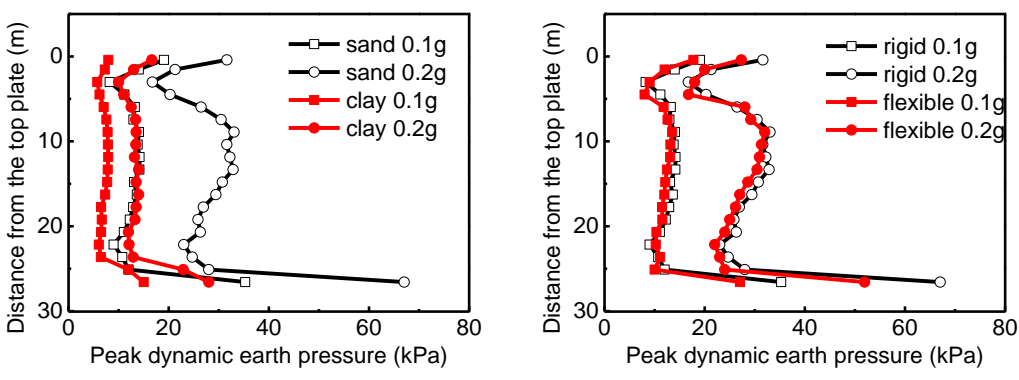


Figure 10. Influences of (a) soil type and (b) stiffness of structure

## Stiffness of the structure

The diaphragm wall is 1.2 m wide. Dimensions of the inside wall vary from 0.4 m to 0.8 m (from top to bottom). The original structure with diaphragm wall was defined as a rigid structure while the structure without diaphragm wall was regarded as a flexible one. The lateral stiffness of the wall consist of the diaphragm wall and the inside wall on the bottom story was about 16 times the stiffness of the wall of the flexible one. Figure 10 shows the difference between the rigid structure and the flexible structure. It is seen that peak dynamic earth pressure of the flexible one was a little smaller than that of the rigid one whether under a small or large earthquake. But the difference was small. Properties of soils had more influences on dynamic earth pressure than stiffness of the structure.

# Vertical earthquake

To study influence of vertical earthquake component on the dynamic earth pressure, peak vertical acceleration was scaled to be 2/3 of peak horizontal acceleration. Figure 11 presents the peak dynamic earth pressure under two levels of the earthquake with and without vertical component. Specifically, when peak horizontal acceleration was 0.1 g, average values of peak dynamic earth pressure with and without vertical component were 13.93 kPa and 17.77 kPa, respectively. Values were 29.39 kPa and 34.99 kPa when peak horizontal acceleration was 0.2 g. Hence, vertical earthquake component excited lateral dynamic earth pressure.

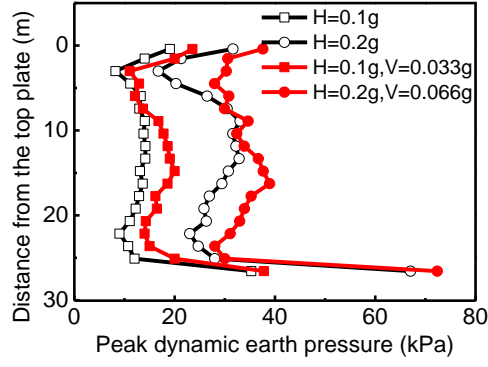


Figure 11. Influences of vertical earthquake component

## **Conclusions**

In this paper, to study distributions and amplitudes of dynamic earth pressure along the side wall of an underground subway station, a series of 1-g shaking table tests were conducted on a four-story subway station firstly. Experimental results were used to confirm the reliability of the numerical technique. Then parametric study was carried out through nonlinear dynamic time history analyses using the general purpose finite element code ABAQUS. The following conclusions are drawn from the results of the study.

- (1) The distribution of peak lateral dynamic earth pressure appeared an "S" shape, which was distinguished from that of a single-story underground structure. Different type of ground motions had influences on amplitudes of pressure, but distribution shapes were similar. And with the increase of the magnitude of the earthquake, dynamic earth pressure increased remarkably
- (2) At the lower part of the structure, ratios of dynamic to static earth pressure were similar. Specifically, when the peak horizontal acceleration was 0.2 g, lateral earth pressure on the lower part of the structure increased nearly thirty percent, which needed attention in practice. And vertical earthquake component excited lateral dynamic earth pressure.
- (3) Properties of soils had more influences on dynamic earth pressure than stiffness of the structure. Structures surrounded by sand suffered larger dynamic earth pressure than that by clay. Peak dynamic earth pressure of the flexible structure was a little smaller than that of the rigid one whether under a small or large earthquake, but the difference was small.

## Acknowledgements

This research was supported by the State Key Laboratory of Disaster Reduction in Civil Engineering (SLDRCE14-B-11), National Natural Science Foundation of China (Grant No. 51278524), and Innovation Program of Shanghai Municipal Education Commission (14ZZ034). All support is gratefully acknowledged.

#### Reference

- Chen, Z. Y., Chen, W., Li, Y. Y., and Yuan, Y. (2015) Seismic performance of central columns for a multi-story subway station under vertical earthquake excitations, *Engineering structures* (submitted)
- Gazetas, G., Psarropoulos, P., Anastasopoulos, I., and Gerolymos, N. (2004) Seismic behaviour of flexible retaining systems subjected to short-duration moderately strong excitation, *Soil Dynamics and Earthquake Engineering* **24**, 537–550.
- Luu, A. L. (2013) Seismic earth pressures measured during a shake table experiment of underground structures. University of California, Irvine.
- Madabhushi, S., and Zeng, X. (2007) Simulating seismic response of cantilever retaining walls, *Journal of geotechnical and geoenvironmental engineering* **133**, 539–549.
- Ostadan, F. (2005) Seismic soil pressure for building walls: An updated approach, *Soil Dynamics and Earthquake Engineering* **25**, 785–793.
- Psarropoulos, P., Klonaris, G., and Gazetas, G. (2005) Seismic earth pressures on rigid and flexible retaining walls, *Soil Dynamics and Earthquake Engineering* **25**, 795–809.
- Sun C. F. (2013) Approving of numbers of urban railway projects which reach four trillion by 2020, *Sichuan Cement* **07**, 72–73 (In Chinese)
- Wang, W. P., Tao, L. J., Zhang, B., Li, W. B., and Wei, Y. J. (2010) A New Method for Seismic Active Pressure Calculation of the Underground Structure, *Journal of Disaster Prevention and Mitigation Engineering* **30**, 620–623.
- Yang, L. D., Yang, C., and Ji, Q. Q. (2003) Shaking table test and numerical calculation on subway station structures in soft soil, *Journal of Tongji University* **31**, 1135–1140.